Solubility Validation from Boildown Data for Hanford Tank Liquids - 14445

S. F. Agnew*, R.A. Wilson*, W.G. Ramsey**

*Columbia Energy and Environmental Services, Inc., 1806 Terminal Dr., Richland, WA 99354
**Washington River Protection Solutions, Richland, WA 99354

ABSTRACT

Space in Hanford waste tanks is very limited and therefore active evaporation of tank liquids continues to provide a means to recover tank space. Prior to each evaporator campaign, a boildown of a sample of tank liquid provides a basis for planning by measuring density, solids precipitation, and water activity as a function of concentration. We have found these datasets also provide opportunities to validate and calibrate various solubility models on actual waste.

Boildown studies for liquids from five tanks and tank blends have been reported from Hanford's 222-S laboratory. Notably, solutions were assayed and solid phases determined for each of many concentration points. While $NaNO_3$ was the dominant precipitate and determined the endpoint concentration for each boildown, other solids that precipitated were $NaNO_2$, $Na_2CO_3.H_2O$, Na_2SO_4NaF, $Na_3PO_4(NaF.19H_2O)_{0.5}$, $Na_3PO_4.12H_2O$, and $Na_2C_2O_4$. Importantly, though, no $Al(OH)_3$ solids ever precipitated during any of these boildowns despite model predictions for limited Al solubility.

This paper will show that while thermodynamic models are useful for general predictions of solubility, the kinetics of crystal growth and salting effects as well as solution speciation are also important considerations, especially for Al. An Al solubility model suggests that Al persists supersaturated for many months in some of these tank liquids. In addition, the kinetic effects of $NaNO_3$ precipitation often induced some $NaNO_2$ and $Na_2CO_3.H_2O$ co-precipitation despite thermodynamic predictions that these species were not saturated.

INTRODUCTION

The recovery of tank space by means of active evaporation of waste liquids has been a very common function at Hanford for over fifty years. While in the past only minimal studies were performed on tank liquids prior to concentration, more recent waste reduction campaigns have been preceded by much more detailed boil-down studies [1-5] for each campaign.

This paper will show how these detailed boil-down studies are a very valuable means to calibrate solubility models for various waste species. At some point during concentration, each of the electrolytes precipitate and therefore provide a basis for validating model predictions. The phosphate-fluoride double salt, for example, was saturated even in the initial solutions. In contrast, there were no Al solids that formed during any of the boildown tests. Aluminum precipitates as the neutral $Al(OH)_3$ despite being an electrolyte in solution as aluminate, $Al(OH)_4^-$ and various solubility models predict that Al should precipitate in many of these samples.

We will show how these boildown datasets are consistent with a simple phosphate-fluoride solubility model previously proposed and that aluminum supersaturation occurs upon cooling for some of the samples.

METHODOLOGY

Previous reports describe [1-5] the detail of liquid samples from five different tanks and tank blends and only the salient features are described here. Samples from five different tanks and tank blends were evaporated at three constant pressures of 40, 60, and 80 torr until an excess of 20 vol% solids precipitated. The temperature varied accordingly from 40-60°C during each boildown and resulted in precipitation of various minor solids very early and eventually major electrolytes precipitated, usually $NaNO_3$ and Na_2CO_3.

An example of the major species concentrations appear in Fig. 1 and minor species in Fig. 2, both as a function of free hydroxide for AP-105. Free hydroxide is a convenient metric of the concentration since it does not result in any precipitates and is therefore proportional to volume reduction. Each boildown consisted of 6-10 assays of extracts from the bottoms during the boildown. Extracted samples were cooled to 18°C for five days and then assayed for liquid composition and solids phase identification.

Figure 1. Major species molarities for boildown of AP-105.

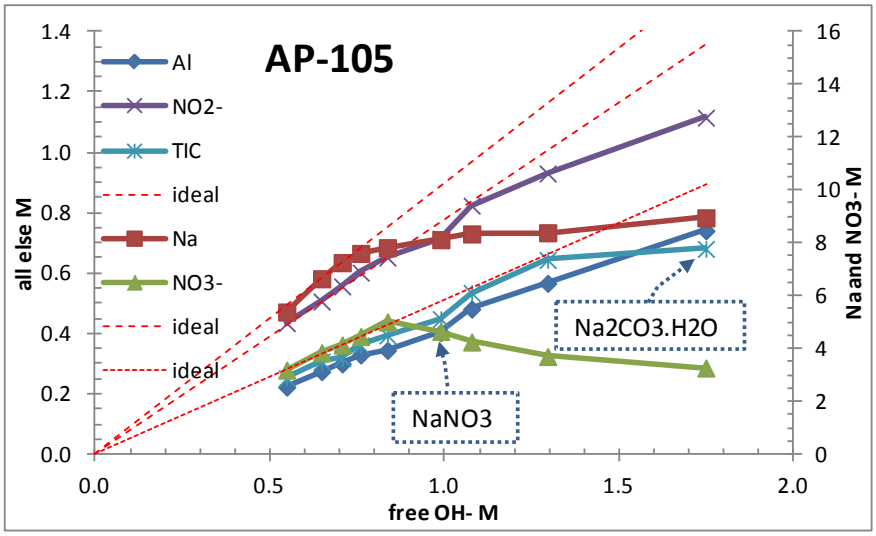

Concentration of major species versus free hydroxide for the boildown of a sample of AP-105. Species that deviate from the dashed ideal lines have precipitated.

The ideal lines in Figs. 1 and 2 are extrapolations of the ideal concentrations for species given the volume concentration.

Figure 2. Concentrations of minor species for boildown of AP-105.

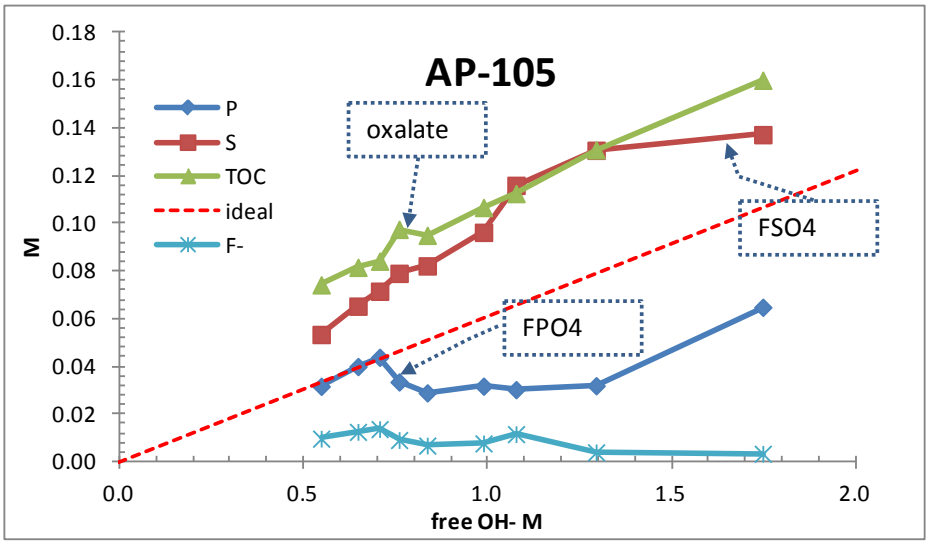

Minor species concentrations versus free hydroxide for boildown of AP-105. Deviations from the dashed ideal line indicate precipitation of phosphate as $Na_3PO_4.(NaF.19H_2O)_{0.5}$ and $Na_2SO_4.NaF$ precipitates from its ideal line (not shown) as well. Plot shows phosphate as P and sulfate as S.

Vapor pressures were kept constant relative to absolute barometric pressure and were therefore water activities. Each boildown measured solution vapor pressure ratio with the vapor pressure of pure water at temperature given the Antoine equation of state for water [6].

Water Activity by Solvation Cluster Equilibria

Precipitated solids with waters of hydration depend on the activity of water and both phosphate and aluminate solubilities therefore depend on water activity. Aluminum solubility depends on the equilibrium between aluminate and its dimer, which in turn depends on water activity as well as on the entropy of mixing due to the complexity of the solution mixture. To estimate water activity, we used the solvation cluster equilibria (SCE) model [7] with parameters K and n fitted to the mixtures with linear regression.

$$a_w = \frac{1}{1+\frac{\sum \nu_i m_i}{55.51}+\gamma_{mix}\left(\frac{1}{1+\frac{55.51}{\sum \nu_i m_i}}\right)^n \prod \left(K_i \gamma_{iDH}\right)^{f_i n_i}} \qquad \text{(Eq. 1)}$$

K_i = SCE hydration equilibrium constant
n_i = SCE hydration order, m_i is molality of electrolyte i
ν_i = the SCE effective ion number for electrolyte i
f_i = fraction of electrolyte I
γ_{iDH} = Debye-Hückel factor (no parameters)

γ_{mix} = entropy of mixing factor (no parameters)
$n = \Sigma\ f_i\ n_i$, weighted average n, hydration order

For the Hanford tank waste liquids, we have fit K_i and n_i for each of NaOH, $NaAl(OH)_4$, $NaNO_3$, and $NaNO_2$ by least squares regression to the water activity data.

Solubility of $Al(OH)_3$

The solubility of aluminum in Hanford waste liquids depends on hydroxide, water activity, and mixture complexity described previously [8]. Aluminum solubility in complex electrolytes has been the subject of many previous reports and has been thoroughly reviewed [ref cited in 8].

In its simplest form, gibbsite, bayerite, or $Al(OH)_3$ solubility is

$$Al(OH)_3(solid) + OH^- <> Al(OH)_4^- \qquad \text{(Eq. 2)}$$

and this expression shows up in much previous work.

We use the dimer dSmix (DDS) model as described previously [7] to calculate Al solubility for these boildowns. The DDS model also incorporates the aluminate dimer, water activity, and the entropy of mixing to provide a more comprehensive aluminum solubility that is consistent with a wide range of complex Al mixtures.

Solubility of $Na_3PO_4[NaF.19H_2O]_{0.5}$

A straightforward solubility product for phosphate fluoride double salt was used [9]

$$C_{PO4} = e^{-4911.4(1/T-1/298.15)} * 0.025 / \{C_{Na}^{0.91906} * C_{OH}^{0.11309} * C_F^{0.31445}\} \quad \text{(Eq. 3)}$$

where

T, temperature in Kelvin
C_{Na}, molal Na^+ concentration
C_{OH}, molal OH^- concentration
C_F, molal fluoride concentration
C_{PO4}, molal phosphate concentration
a_w, water activity.

A more sophisticated solubility product that incorporates an equilibrium between two solution species for phosphate, one with and one without fluoride dependence, results in a more complex form that also includes water activity as

$$C_{PO4} = e^{-4911.4(1/T-1/298.15)} * 0.055 / \{C_{Na}^{4.09} * C_{OH}^{1.89} * C_F^{1.61} * a_w^{4.46} / (153/C_{Na} + 1) + C_{Na}^{-0.287} * C_{OH}^{-0.189} * a_w^{-0.926} * [1 - 1/(153/C_{Na} + 1)]\} \quad \text{(Eq. 4)}$$

Ion Balance

It is important that the solution compositions show ion balance since fitting parameters to solutions with ion balance errors results in fits that reflect those errors. There are many

uncertainties and systematic errors in solubility modeling and ion balance is one of the many sources of uncertainty. We have therefore balanced the ions with a simple expedient of adjusting cations and ions to their averages. Figure 3 lists the ion balances from the progression of each boildown.

Although ion balance can be off due to either or both cation and anion measurements, we have assumed that both cation and anion measurements are equally in error. This means that cations are adjusted as

$$C_{Na} = C_{Na} * (1 + C_{anions} / C_{cations}) / 2$$

while anions are adjusted as

$$C_{NO3} = C_{measNO3} * (1 + C_{cations} / C_{anions}) / 2 \ .$$

Figure 3. Ion balance over all boildown assays.

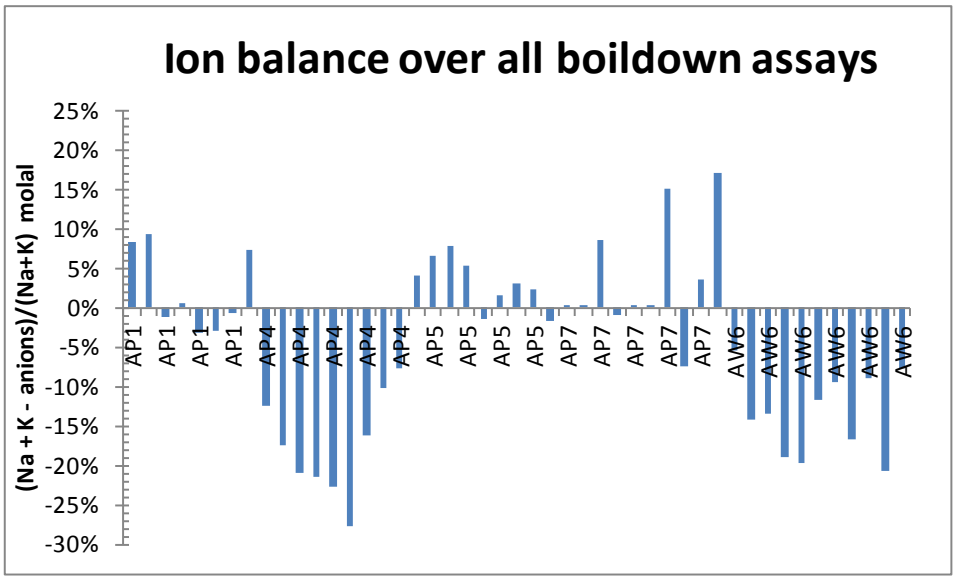

Ion balances for all assays in the progression from each boildown. While there appear to be some trends in ion balance, by and large there is no consistent pattern.

RESULTS AND DISCUSSION

Table I shows the initial concentrations for all of the boildowns. The dominant species is nitrate and nitrate is the major precipitate observed in all cases followed by carbonate and then nitrite. However, the minor precipitates of phosphate-fluoride, oxalate, and sulfate-fluoride were also observed for all boildowns. The uncertainties for the boildown assays are discussed in each of the reports. [1-5]

Table I. Starting liquid compositions, M.

Species	AP-101	AP-104 /AW-102	AP-105	AP-107	AW-106
Na^+	4.9	5.3	5.3	4.7	4.4
NO_3^-	2.1	1.2	3.3	1.9	1.8
NO_2^-	0.50	1.2	0.44	0.65	0.71
OH^-	1.3	0.77	0.56	0.58	0.46
$Al(OH)_4^-$	0.20	0.35	0.23	0.16	0.23
$CO_3^=$	0.30	0.58	0.26	0.48	0.39
PO_4^{3-}	0.035	0.048	0.032	0.030	0.035
$SO_4^=$	0.037	0.032	0.054	0.096	0.081
TOC	0.083	0.28	0.076	0.11	0.11
F^-	0.043	0.012	0.0010	0.024	0.019
Cl^-	0.037	0.10	0.040	0.039	0.049
K^+	0.28	0.065	0.030	0.035	0.045

Water Activity by Solvation Cluster Equilibria

Regressing the SCE parameters with two parameters for each species NaOH, $NaAl(OH)_4$, $NaNO_3$, and $NaNO_2$ resulted in fit shown in Table II and Fig. 3 with the measured water activity. Although previous work had derived parameters for water activity from pure electrolyte solutions, these SCE parameters were simply fit in a least squares sense to the measured water activities for all of these solutions with a correlation coefficient of 0.98.

Table II. Solvation cluster equilibria parameters from regression to boildown data to Eq. 1.

	K_i	n_i	ν_i
NaOH	4.25	1.25	2
$NaAl(OH)_4$	24.1	3.08	2
$NaNO_3$	0.96	1.28	2
$NaNO_2$	0.773	10.69	2

The advantage of the SCE approach for water activity is that it provides a great deal of flexibility for estimating water activity for such complex mixtures as Hanford tank wastes. With just two adjustable parameters for each of four major species, we find the water activity scatterplot, Fig. 3, with a correlation coefficient of 0.98.

Figure 3. Water activity scatterplot, SCE versus measured.

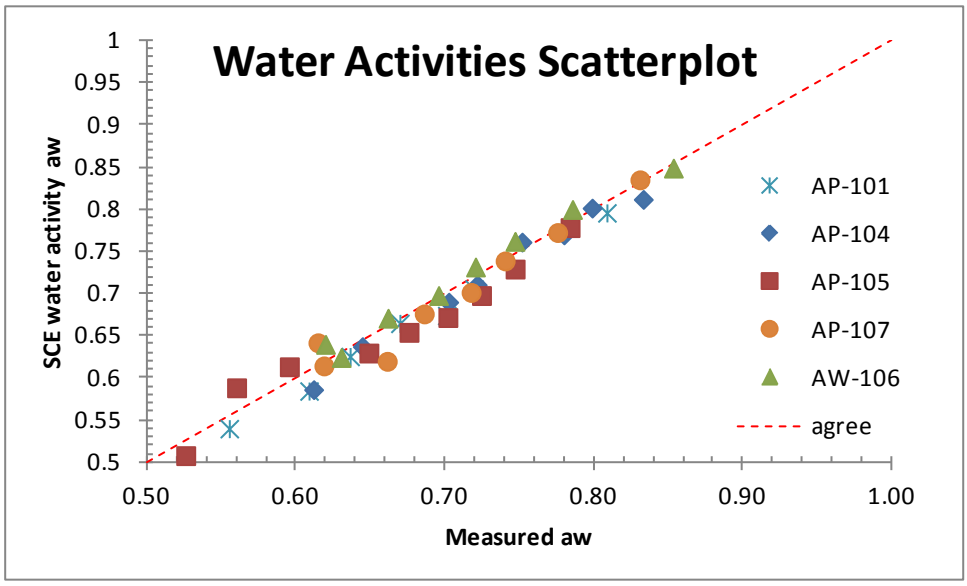

Water activities calculated with the SCE parameters in Table II fit to the measured water activities of the five boildowns shown with a coefficient of 0.98.

Water activity plays a role in each of aluminum and phosphate solubilities, and so it is important to have a reasonable expression for water activity. Since water activity was measured for all of these boildowns, those measured water activities were used for each solubility prediction. Water activity is also related to the solution free energy by means of the Gibbs-Duhem integration and so provides a check on the solution free energy. The solution free energy is very important for predicting the solubilities of the major species.

Solubility of $Al(OH)_3$

All samples have been heated to ~60°C during each of their boildowns as the approximate temperature at which these endpoints boil at 80 torr. The DDS model is consistent with complete solubility of Al at 60°C as shown in Fig. 4 and the prediction of the DDS model is that Al would be completely soluble in all cases under these conditions.

Figure 4. Measured versus DDS Al solubility at 60°C.

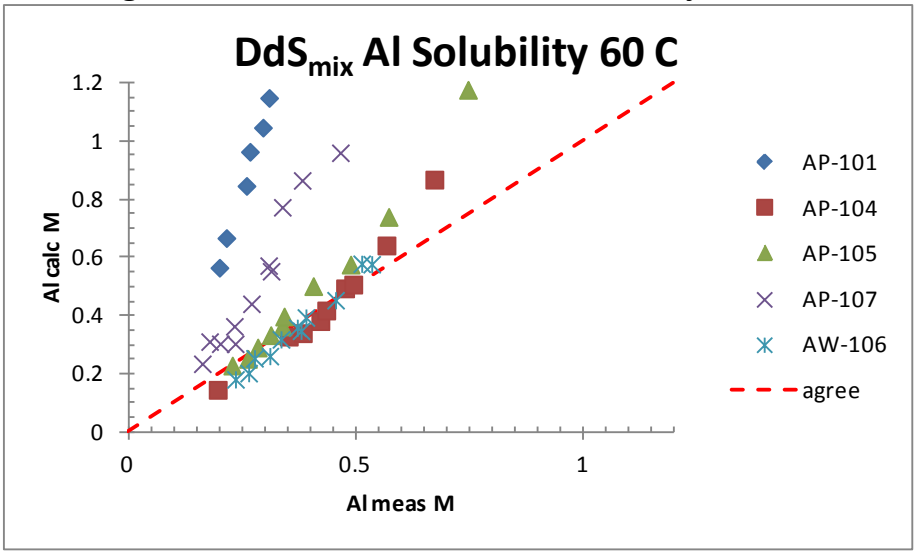

Predictions for DDS model Al solubility at 60°C versus measured Al at 18°C for all solutions of the boildowns. Aluminum solubilities measured at 18°C appear consistent with solutions at 60°C.

Once all of the $Al(OH)_3$ is dissolved, the supersaturation of Al is well known for solutions that do not contact any gibbsite seed [11-13]. Upon cooling to 18°C, three of the five solutions should have shown Al precipitation by the DDS model as shown in Fig. 5. The lack of Al precipitate in any of these solutions suggests that they were supersaturated in Al upon cooling to 18°C and were therefore only metastable. The temperature dependence of the DDS model comes from fitting Al solubilities up to 120°C as reported previously [7].

Figure 5. Measure versus DDS Al solubility at 18°C.

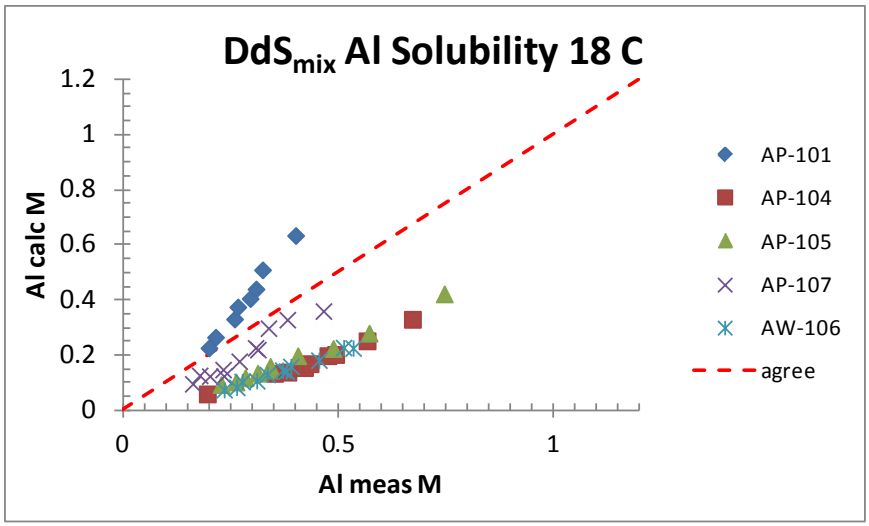

Plot of DDS Al solubility predictions versus measured in M for the five boildown runs as indicated at 18°C. Points above the dashed line indicate unsaturated Al solutions while those below the dashed line are supersaturated in Al.

Solubility of $Na_3PO_4[NaF.19H_2O]_{0.5}$

The phosphate-fluoride double salt was a very common minor precipitate [10] that showed up in all boildowns and was saturated in nearly all solutions at 18°C. In contrast to the phosphate-fluoride, there were never any Al precipitates observed in any of the samples at 18 °C.

The phosphate-fluoride double salt in Fig. 6 shows the measured phosphate concentrations data versus a simple phosphate solubility model that has been derived for Hanford tank liquids [9]. Although the correlation coefficient is only 0.51 for this scatterplot, this accuracy may be sufficient for some applications.

Note that there are some systematic deviations in phosphate apparent among these datasets. Datasets for AP-104 and AW-106, for example, suggest that there may be solution speciation for the phosphate and/or fluoride ions in solution. The more complex phosphate solubility of Eq. 4 does show a better correlation coefficient of 0.74 as shown in Fig. 7.

Note the presence of an apparent phosphate outlier in the Figs. 6 and 7 for the endpoint of AP-105 boildown. The phosphate solubility at about 0.06 M is in excess of the starting phosphate solubility shown in Fig. 2 for AP-105. Associated with that increase in phosphate, there is a concomitant decrease in sulfate solubility due to precipitation of the sulfate-fluoride double salt. This measurement suggests that there may be more complex interactions between phosphate and sulfate solids in Hanford's future sludge washing, but since this outlier is just one point, more data is needed to validate this correlation.

Figure 6. Calculated and measured phosphate molar concentrations.

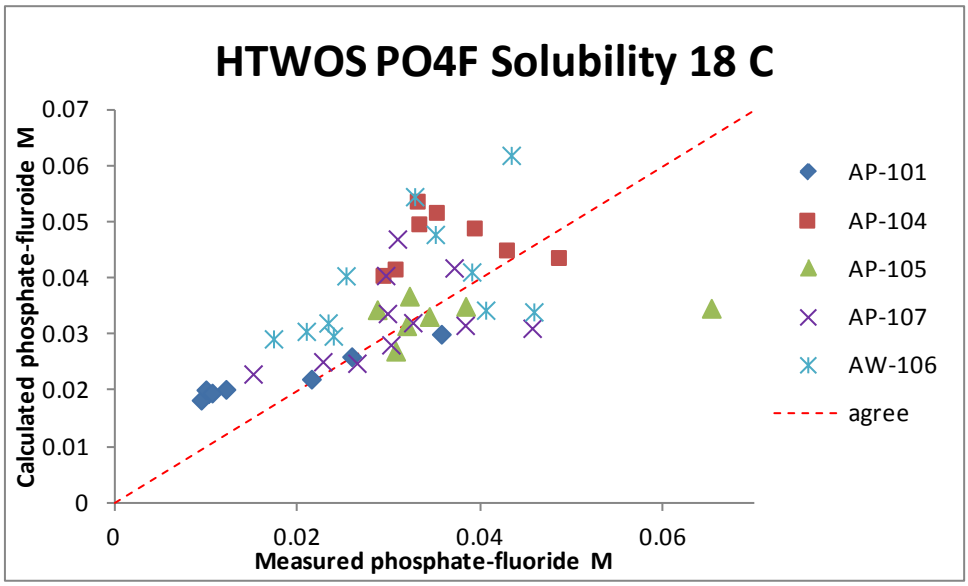

Scatter plot of measured phosphate versus predicted phosphate solubility by Eq. 3 in text. The boildown data appear to be consistent with the simple phosphate model developed for the HTWOS simulation with a correlation coefficient of 0.51.

Solubility of $NaNO_2$

When more than one species precipitates at the same time, a ternary or the more general multinary precipitation, the relative amounts of species depend on both equilibrium solubility and the kinetics of crystal growth. While the solution free energy changes with the precipitation of both solids, the kinetics of precipitation of one solid can either enhance or suppress the precipitation of another solid in a process known as salting out or salting in, respectively.

These salting effects due to coprecipitation kinetics can be quite complex and highly dependent on the evaporation rate [14]. For example, the carbonate/sulfate double salt burkeite, $Na_2CO_3[Na_2SO_4]_2$ has been extensively studied in simulated waste evaporates [14] with very similar compositions to these actual wastes, but burkeite was not observed in any of these actual waste boildowns despite the similarity in compositions.

As an example of salting out, nitrite precipitation occurs for AP-105 at a concentration that is well below the nitrite-nitrate triplepoint [15, 16]. This suggests that nitrite precipitation is not at equilibrium but rather is a kinetic precipitate likely associated with nitrate precipitation. For each of the boildowns in Table II, the concentrations of nitrite are equal for one and substantially lower than nitrate for the others. However, the nitrite-nitrate triplepoint is reported [15, 16] to be where nitrite is ~1.5 times nitrate concentration.

The major species begin precipitating $NaNO_3$ followed by $NaNO_2$ and then $Na_2CO_3.H_2O$. The simultaneous presence of two or more solids represent ternary, or more generally, multinary points in the equilibrium phase diagrams. However, previous work shows [9,10] that nitrite

should not precipitate from any of these boildowns. The nitrite concentration at the nitrate/nitrite multinery point should be ~1.8 times more soluble than nitrate and so solid nitrite should not coexist with solid nitrate for any of these boildowns. The co-precipitation of $NaNO_2$ with $NaNO_3$ is apparently a kinetic precipitation most likely due to the dominant precipitation of $NaNO_3$ providing nucleation for $NaNO_2$ as well. Although most pronounced for AP-105, coprecipitation of $NaNO_2$ with $NaNO_3$ occurred to some extent for each of the boildowns.

These kind of kinetic effects have been reported for the double salt burkeite, where a kinetic precipitation has been observed in evaporated actual and simulated wastes [14]. Burkeite, though expected, has not been observed in any of the AP tank saltcakes and as well as many other saltcakes [17].

The minor species that precipitate are phosphate-fluoride and sulfate-fluoride double salts as well as oxalate, all solids of which were identified with a combination of PLM, SEM/EDX, and XRD analyses on the solids. The precipitation of these minor species has little effect on the solution free energy and as a result, minor species tend to show simpler dependencies as solubility products.

Figure 7. Calculated and measured phosphate molar concentrations.

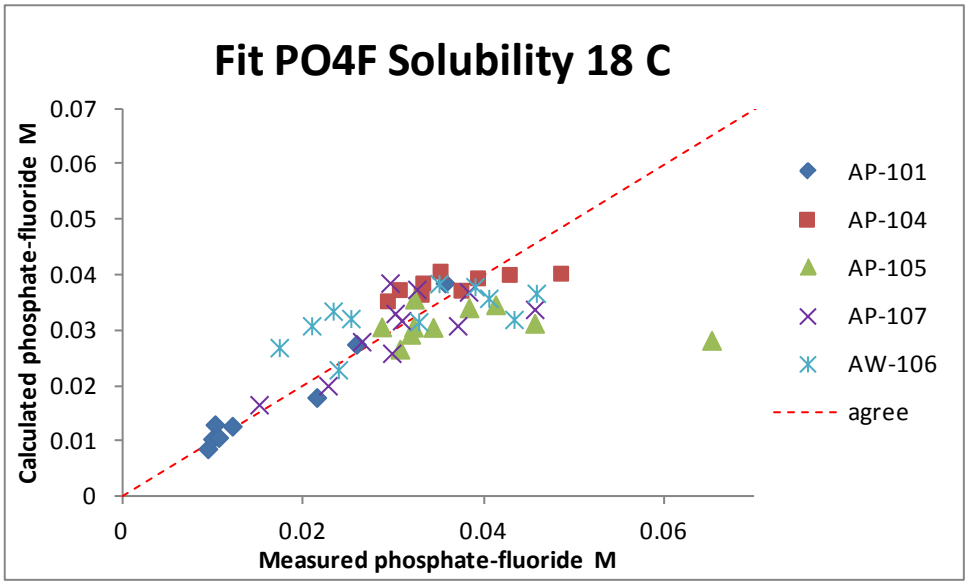

Scatterplot of measured phosphate versus predicted phosphate solubility by Eq. 4 in text. The boildown data appear to better correlate with this more complex phosphate model with a correlation coefficient of 0.74.

SUMMARY

Recent boildowns provide a great deal of data on the compositions of real waste solutions as well as on the speciation of precipitates from these solutions upon concentration. These very useful

datasets permit the validation of equilibrium solubility models for complex electrolyte mixtures as well as provide kinetic and speciation information that complements equilibrium solubilities.

In the case of Al solubility, the dimer-dS_{mix} (DDS) model is a relatively simple thermodynamic model that is consistent with reported aluminum solubility over very wide ranges of compositions and temperatures [8]. At 60°C, the DDS model predicts Al solubility for all boildown solutions, but once these solutions are cooled to 18°C, three solutions should have precipitated Al solids and yet none of the solutions showed any Al solids nor any loss of Al from solution.

In fact Al supersaturation is a very well known phenomenon in the absence of gibbsite seeds and typically, the Bayer process for manufacturing gibbsite facilitates Al precipitation by addition of gibbsite seed crystals to Al supersaturates [11-13]. We suggest that a gibbsite strike for the boildown solutions in the future would quantify this supersaturation and further validate the DDS or any other Al solubility model. Preliminary planning is now underway to incorporate this strike in future boildown studies.

The solubility of the phosphate-fluoride double salt seems to be consistent with a simple solubility model that has been proposed for the HTWOS modeling effort and further studies are underway to validate solubility models for the other species involved as well. For example, the more sophisticated solubility expression may prove to be more useful.

The precipitates for these concentrates are mixtures of the major electrolytes $NaNO_3$, Na_2CO_3, and $NaNO_2$. When two or more electrolytes are in equilibrium with a saturated liquid, this should represent an invariant multinary point in the phase diagram with unique concentrations. However, the kinetics of nucleation and crystal growth along with the presence of multiple soluble species mean that these multinary points will vary, sometimes markedly.

Therefore it is important to calibrate a solubility model for a complex mixture with a set of assays from samples that reflect the kinetics of either precipitation for the case of evaporation or dissolution for the process of washing or leaching.

The quality assurance for this paper is consistent with current policy for the application intended.

ACKNOWLEDGEMENTS

Thanks to Washington River Protection Solutions, LLC and Columbia Energy and Environmental Services, Inc. for support of this project.

REFERENCES

1. Callaway, W.S., “Results of Boildown Study on Liquid Waste Retrieved from Tank 241-AW-106”, WRPS-1000136, January 2010.

2. Callaway, W.S. “Final Results of Boildown Study on Supernatant Liquid Retrieved from Tank 241-AP-105,” 7S110-WSC-07-143, December 2007.
3. Callaway, W.S., J. S. Page, “Boildown Study on Supernatant Liquid Retrieved form AP-107,” LAB-RPT-12-00008, Rev. 0, January 2013.
4. Callaway, W.S. “Final Results of Boildown on Supernatant Liquid Retrieved from Tank 241-AP-101,” 7S110-WSC-08-145, February 2008.
5. Callaway, W.S. “Final Results of the Boildown Study Supporting 242-A Evaporator Campaign 07-01,” 7S110-WSC-07-110, April 2007.
6. Antoine, C. "Tensions des vapeurs; nouvelle relation entre les tensions et les températures", Comptes Rendus des Séances de l'Académie des Sciences 107: 681–684, 778–780, 836–837, 1888.
7. Agnew, S.F., C.T. Johnston, “Aluminum Solubility in Complex Electrolytes”, Proceedings of Waste Management Conference, Feb. 24-28, Phoenix, AZ, 2013.
8. Agnew, S.F., J.G. Reynolds, C.T. Johnston, “Predicting Water Acitivity for Complex Wastes with Solvation Cluster Equilibria (SCE),” Proceedings of Waste Management Conference, Feb. 26 - Mar. 1, Phoenix, AZ, 2012.
9. Belsher, J.D., P.A. Empey, T.M. Hohl, R.A. Kirkbride, F.L. Meinert, J.S. Ritari, K.R. Seniow, E. B. West, “Hanford Tank Waste Operations Simulator (HTWOS) Version 6.6.1 Model Design Document,” RPP-17152, Rev. 6, September 2011.
10. Reynolds, J.G., G.A. Cooke, D.L. Herting, R. W. Warrant, “Salt Mineralogy of Hanford High-Level Nuclear Waste Staged for Treatment,” Indus. Eng. Res. 152, 9741-9751, 2013.
11. Walker, D.D., “Stability Tests with Actual Savannah River Site Radioactive Waste,” WSRC-TR-2002-00026, 2002.
12. Addai-Mensay, J., A. Gerson, C.A. Prestidge, I. Ametov, J. Ralston, “Interactions between Gibbsite Crystals in Supersaturated Caustic Aluminate Solutions,” Light Metals, B. Welch, Ed., 159-166, 1998.
13. van Straten, H.A., P.L. de Bruyn, “Precipitation from Supersaturated Aluminate Solutions,” J. Coll. Interface Sci, 102, 260-277, 1984.
14. Nassif, L., “Accelerating Treatment of Radioactive Waste by Evaporative Fractional Crystallization”, Ph.D. Thesis, Georgia Institute of Technology, May 2009.
15. Seidell, A. “Solubilities of Inorganic and Organic Compounds,” D. van Nostrand, New York, NY, 1919
16. Reynolds, D.A., D.L. Herting, “Solubilities of Sodium Nitrate, Sodium Nitrite, and Sodium Aluminate in Simulated Nuclear Waste,” RHO-RE-ST-14P, September 1984.
17. Herting, D.L., G.A. Cooke, R.W. Warrant, “Identification of Solid Phases in Saltcake from Hanford Site Waste Tanks,” HNF-11585, Rev. 0, September 2002.